

associated with UO_2^{2+} ions in majority and minority sites within the crystal. The luminescence is assigned to the $\Sigma_g^+ \leftarrow \Pi_g$ emissive transition origin, and to vibronic lines associated with this origin. Those vibronics associated with quanta of the symmetric stretching mode of UO_2^{2+} (ν_1) are strongly circularly polarized, while those that include quanta of asymmetric stretching or bending modes are essentially unpolarized. This behavior is rationalized in terms of a model of vibronic optical activity presented in the Results

and Analysis section. Special consideration was given to the origin region of the $\Sigma_g^+ \leftarrow \Pi_g$ transition. The origin transition associated with the majority (B-site) UO_2^{2+} species shows interesting chiroptical behavior associated with circular dichroic self-absorption.

Acknowledgment. This work was supported by a grant from the National Science Foundation (CHE-8820180 to F.S.R.).

Registry No. $\text{Na}[\text{UO}_2(\text{CH}_3\text{COO})_3]$, 17712-38-8.

Contribution from the Department of Chemistry,
North Dakota State University, Fargo, North Dakota 58105-5516

Hypercoordination in Group IV MH_5 and MH_5^- Systems

Marshall T. Carroll, Mark S. Gordon,* and Theresa L. Windus

Received July 17, 1991

The energetics and bonding of the group IV hypervalent MH_5 and $\text{MH}_5^- D_{3h}$ structures ($M = \text{C}, \text{Si}, \text{Ge}, \text{Sn}$) are examined in this paper. Ab initio all-electron calculations are used to predict the energies and geometries of the systems. The resulting electron densities are analyzed using the topological theory of atoms in molecules. It is found that the anion energetically is more stable than the neutral radical for $M = \text{Si}, \text{Ge},$ and Sn but not for $M = \text{C}$. Further distinguishing carbon from the other members of the group is the fact that the CH bond mostly is of covalent character while the other MH bonds are mostly of ionic character. Scrutinizing difference density maps and atomic property changes reveals that, upon anion formation, the incoming electron density becomes preferentially accumulated in the nonbonded regions of the axial and, to a lesser extent, equatorial hydrogens.

Introduction

Hypervalent structures (compounds in which a central atom is apparently surrounded by more than the "normal" octet of electrons) are playing an increasingly important role in mechanistic interpretations of observed organosilicon chemistry. The simplest prototypical hypervalent silicon species is SiH_5^m , where m can be negative (anion), positive (cation), or neutral. Many theoretical papers have addressed the nature of the structure and bonding in SiH_5^- .¹⁻⁷ In a recent paper, Maitre and co-workers have used a valence bond model to account for the energy differences between SiH_5 and SiH_5^- (D_{3h} symmetry) and to explain the fact that the anion is a local minimum, while the neutral species apparently is not.¹ The essence of their analysis is that an ionic model is not sufficient for the description of SiH_5^- . This is in contrast to the ionic model that has been used to describe the electronic structure of SiH_4F^- .⁸

The SiH_5^- anion has been theoretically¹⁻⁷ and experimentally^{9,10} characterized as a hypercoordinated species having D_{3h} symmetry. Even though the radical SiH_5 is predicted to be higher in energy than the anion,¹ the radical recently has been observed in an ESR spectrum,¹¹ as has its Group IV analogue GeH_5 .¹² A theoretical

investigation (at the unrestricted Moller-Plesset second-order perturbation level of theory at the restricted open-shell Hartree Fock geometry using a double- ζ basis set) has predicted that GeH_5 is an unstable transition state.¹³ The lightest group IV hypervalent species, CH_5 and CH_5^- , have both been predicted to be unstable transition states with the radical energetically more stable than the anion.^{6,10,14-16} To our knowledge, the corresponding tin systems, SnH_5 and SnH_5^- , have not yet been investigated.

In the present paper we use ab initio all-electron calculations to predict the structures and energies of group IV MH_5 and MH_5^- systems, for $M = \text{C}, \text{Si}, \text{Ge},$ and Sn . The theory of atoms in molecules¹⁷ is employed to examine the nature of the bonding in these compounds.

The principal questions addressed in this paper are as follows:

- (1) Does the fundamental nature of the M-H bond vary as a function of M, and if so, in what way?
- (2) Why is SiH_5^- energetically more stable than SiH_5 , while the opposite is true for $M = \text{C}$?
- (3) In what manner does the total electron distribution change upon addition of an electron to the radical to form the anion?
- (4) How do the properties of MH_4 change upon addition of H or H⁻ to form products?

Computational Approach

Ab initio all-electron calculations were performed using GAMESS.¹⁸ Restricted Hartree-Fock (RHF) and restricted open-shell Hartree-Fock

- (1) Maitre, P.; Volatron, F.; Hiberty, P. C.; Shaik, S. S. *Inorg. Chem.* **1990**, *29*, 3047.
- (2) Sini, G.; Ohanessian, G.; Hiberty, P. C.; Shaik, S. S. *J. Am. Chem. Soc.* **1990**, *112*, 1407.
- (3) Gordon, M. S.; Windus, T. L.; Burggraf, L. W.; Davis, L. P. *J. Am. Chem. Soc.* **1990**, *112*, 7167.
- (4) Burggraf, L. W.; Davis, L. P.; Gordon, M. S. *Top. Phys. Organomet. Chem.* **1989**, *3*, 75.
- (5) Reed, A. E.; Schleyer, P. v. R. *Chem. Phys. Lett.* **1987**, *133*, 553.
- (6) Baybutt, P. *Mol. Phys.* **1975**, *29*, 389.
- (7) Wilhite, D. L.; Spialter, L. *J. Am. Chem. Soc.* **1973**, *95*, 2100.
- (8) Gronert, S.; Glaser, R.; Streitwieser, A. *J. Am. Chem. Soc.* **1989**, *111*, 3111.
- (9) Hajdasz, D. J.; Squires, R. R. *J. Am. Chem. Soc.* **1986**, *108*, 3139.
- (10) Payzant, J. D.; Tanaka, K.; Betovski, L. D.; Bohme, D. K. *J. Am. Chem. Soc.* **1976**, *98*, 894.
- (11) Nakamura, K.; Masaki, N.; Sato, S.; Shimokoshi, K. *J. Chem. Phys.* **1985**, *83*, 4504.

- (12) Nakamura, K.; Masaki, N.; Okamoto, M.; Sato, S.; Shimokoshi, K. *J. Chem. Phys.* **1987**, *86*, 4949.
- (13) Moc, J.; Rudzinski, J. M.; Ratajczak, H. *Chem. Phys. Lett.* **1990**, *173*, 557.
- (14) Dedieu, A.; Veillard, A. *J. Am. Chem. Soc.* **1972**, *94*, 6730.
- (15) Morokuma, K.; Davis, R. E. *J. Am. Chem. Soc.* **1972**, *94*, 1060.
- (16) Niblaeus, K.; Roos, B. O.; Siegbahn, P. E. M. *Chem. Phys.* **1977**, *26*, 59.
- (17) Bader, R. F. W. *Atoms in Molecules: A Quantum Theory*; Clarendon Press: Oxford, England, 1990; and references therein.
- (18) Schmidt, M. W.; Baldridge, K. K.; Boatz, J. A.; Jensen, J. H.; Koseki, S.; Gordon, M. S.; Nguyen, K. A.; Windus, T. L.; Elbert, S. T. *QCPE Bull.* **1990**, *10*, 52.

Table I. Energies and Energy Differences for MH_5 and MH_5^- Systems^a

M	$E(MH_5)$	$E(MH_5^-)$	$\Delta E(I)^b$	$\Delta E(II)^c$	$\Delta E(III)^d$
C	-40.60274	-40.58903	+8.6 (+7.7)	+61.6 (+61.5)	+62.9 (+61.9)
Si	-291.66884	-291.73879	-43.9 (-41.1)	+38.5 (+37.6)	-12.8 (-10.9)
Ge	-2076.02719	-2076.08666	-37.3 (-36.1)	+37.6 (+37.5)	-7.1 (-6.0)
Sn	-5999.49166	-5999.58295	-57.3 (-60.3)	+36.3 (+41.1)	-28.4 (-26.6)

^a Total energies are in hartrees. Energy differences are in kcal/mol. ΔH values (where the zero-point energies have been scaled by 0.89) are listed in parentheses to the right of the corresponding ΔE value. The total energies for CH_4 , SiH_4 , GeH_4 , SnH_4 , H and H^- are calculated to be -40.20217, -291.23133, -2075.58828, -5999.05068, -0.49880, and -0.48707 hartrees, respectively. The 6-31++G(d,p) basis set was used for the carbon and silicon systems.¹⁹ The 6-41++G(d,p) basis set was used for the germanium systems,²⁰ and the 3-21++G(d,p) basis set was used for the tin compounds.²¹ The RHF level of theory was used for the MH_4 and MH_5^- systems, and the ROHF level of theory was used for the MH_5 systems. ^b $\Delta E(I) = E(MH_5^-) - E(MH_5)$. ^c $\Delta E(II) = E(MH_5) - E(MH_4) - E(H)$. ^d $\Delta E(III) = E(MH_5^-) - E(MH_4) - E(H^-)$.

(ROHF) methods were used for the anions and radicals respectively. The 6-31++G(d,p) basis set was used for the carbon and silicon systems.¹⁹ The 6-41++G(d,p) basis set was used for the germanium systems²⁰ and the 3-21++G(d,p) basis set was used for the tin compounds.²¹ The optimized geometries were restricted to D_{3h} symmetry for the hypercoordinated species and to T_d symmetry for the MH_4 systems. The analytic Hessian (matrix of energy second derivatives) corresponding to each optimized structure was calculated and diagonalized, to determine whether the structure is a minimum (positive definite hessian) or n th-order saddle point (n negative eigenvalues).

The critical points in the charge density and atomic properties were calculated using AIMPACK.¹⁷

According to the theory of atoms in molecules (AIM), a bond critical point (r_b) exists between two atoms if there is a saddle point in the total electron density between the two atoms. At the bond critical point, the gradient of the total electron density vanishes ($\nabla\rho(r) = 0$ at $r = r_b$), and the second-derivative matrix of the electron density has one positive eigenvalue λ_3 (corresponding to the bond axis) and two negative eigenvalues λ_1 and λ_2 (corresponding to the perpendicular transverse axes). The existence of a bond critical point implies the existence of a bond path (the path of maximum electron density with respect to any lateral displacement passing through r_b).

The value of the second derivative matrix at the bond critical point, the Laplacian $\nabla^2\rho(r_b)$, is a measure of the local concentration or depletion of electron density. It can be used to classify atomic interactions as closed-shell (a subset being ionic) if it is positive in sign or shared (a subset being covalent) if it is negative in sign. For a closed-shell interaction, electron density is concentrated to a large extent in the separate basins of the participating atoms. For a shared interaction, electron density is accumulated to a large extent between the bonded nuclei. The reader is referred to ref 17 for further details.

Within the AIM formalism, atoms are defined as regions of real three-dimensional spaces bounded by surfaces of zero flux in the electron density. The atomic properties of interest are the net charge on the atom A, $q(A)$, the first moment $\mu(A)$, and the total energy of the atom in the molecule $E(A)$. The explicit form for the net charge is

$$q(A) = Z_A - N(A)$$

where Z_A is the atomic number of A and $N(A)$ is the electron population of A

$$N(A) = \int \int_A \rho(r) d\tau$$

Thus, the number of electrons contained within an atom in a molecule is calculated by integrating the electron density over the volume occupied by the atom in the molecule. This atomic volume is bounded by surfaces of zero flux in the electron density.

The atomic first moment is given by the expression

$$\mu(A) = - \int \int_A r_A \rho(r) d\tau$$

where r_A is the position vector originating at the nucleus of A. The atomic first moment is a measure of the dipolar polarization of electron density within A. As the magnitude of $\mu(A)$ increases, so do the dipolar polarization of A and the deviation of the electron distribution contained within A from spherical symmetry.

The energy of an atom in a molecule at an equilibrium geometry is given by the expression

$$E(A) = \frac{1}{2} \int \int_A \sum_i \lambda_i \varphi_i \nabla^2 \varphi_i d\tau$$

where λ_i is the occupation number of orbital φ_i . The sum of the atomic energies yields the total energy of the molecule. The reader is referred to ref 17 for more detailed discussions of atomic properties.

Results and Discussion

1. Characterization of Stationary Points. The optimized geometries of all MH_4 T_d systems and all but one of the MH_5^- D_{3h} systems were found to be positive definite. The exception is for CH_5^- , for which diagonalization of the hessian yields one negative eigenvalue, with an imaginary frequency = 1653i cm^{-1} , in agreement with previous studies.^{6,10,14} This imaginary mode corresponds to dissociation to $CH_4 + H^-$.

The radicals CH_5 and GeH_5 each have one negative eigenvalue (imaginary frequencies = 3759i and 2574i cm^{-1} , respectively) in agreement with previous studies.^{13,15,16} These imaginary modes correspond to dissociation to $CH_4 + H$ and $GeH_4 + H$, respectively. For SiH_5 , three negative eigenvalues are found, with imaginary frequencies of 2732i cm^{-1} (A_2'') and 140i cm^{-1} (E'). The A_2'' mode corresponds to dissociation to $SiH_4 + H$ and the two degenerate E' modes correspond mainly to axial hydrogen bends. Moc et al. have recently reported only one negative eigenvalue for SiH_5 at the ROHF/6-31G(d)/ROHF/6-31G(d) level of theory.²² Since this is a somewhat smaller basis set than that used in the current study, we have repeated their calculations. However, we still find three negative eigenvalues, with imaginary frequencies of 2654i cm^{-1} (A_2'') and 51i cm^{-1} (E'). Using UHF and UMP2 instead of ROHF, Maitre et al. find only one negative eigenvalue.²³ It should be noted that there is some spin contamination in the UHF calculation ($\langle S^2 \rangle = 0.800$), suggesting some mixing of the quartet with the doublet state.

A further probe of the UHF vs ROHF Hessian is revealing. The UHF axial Si-H distance (SiH_{ax}) is greater than SiH_{eq} (ROHF) by 0.024 Å while the equatorial Si-H distance (SiH_{eq}) is essentially the same for UHF and ROHF. The lengthening of the axial bond apparently occurs as a result of the mixing in of the quartet state, and this is sufficient to cause the two degenerate imaginary frequencies to vanish. This is verified by calculating the ROHF Hessian at the UHF SiH distance. The result is a single imaginary frequency of 3257i cm^{-1} (A_2''). Diagonalization of the ROHF Hessian matrix for SnH_5 yields two imaginary frequencies (113i cm^{-1} ; E'), corresponding mainly to degenerate axial hydrogen bends.

2. Energies. Total energies are listed in Table I. Also included in this table are the energies of the following reactions:



Note that reaction 1 is not an isogyric reaction. However, we are

(19) For first-row elements: Hehre, W. J.; Ditchfield, R.; Pople, J. A. *J. Chem. Phys.* **1972**, *56*, 2257. Hariharan, P. C.; Pople, J. A. *Theor. Chim. Acta* **1973**, *28*, 213. For second-row elements: Francl, M. M.; Pietro, W.; Hehre, W. J.; Binkley, J. S.; Gordon, M. S.; DeFrees, D. J.; Pople, J. A. *J. Chem. Phys.* **1982**, *77*, 3654. Gordon, M. S.; Binkley, J. S.; Pople, J. A.; Pietro, W. J. *J. Am. Chem. Soc.* **1982**, *104*, 2797.
(20) Binning, R. C.; Curtiss, L. A. *J. Comput. Chem.* **1990**, *11*, 1206.
(21) Binkley, J. S.; Pople, J. A.; Hehre, W. J. *J. Am. Chem. Soc.* **1980**, *102*, 939.

(22) Moc, J.; Rudzinski, J. M.; Ratajczak, H. *J. Mol. Struct. (THEO-CHEM)* **1991**, *228*, 131.

(23) Volatron, F.; Maitre, P.; Pelissier, M. *Chem. Phys. Lett.* **1990**, *166*, 49.

Table II. Internuclear Distances and Bond Critical Point Analyses for MH_4 , MH_5 , and MH_5^- Systems^a

system	$r(MH_{ax})$	$r(MH_{eq})$	$\rho(r_{b(ax)})$	$\nabla^2\rho(r_{b(ax)})$	$\rho(r_{b(eq)})$	$\nabla^2\rho(r_{b(eq)})$
CH_5	1.337	1.079	0.143	-0.169	0.290	-1.102
CH_5^-	1.692	1.062	0.067	0.009	0.309	-1.282
SiH_5	1.592	1.491	0.085	0.154	0.111	0.274
SiH_5^-	1.629	1.524	0.084	0.175	0.102	0.258
GeH_5	1.637	1.529	0.097	0.047	0.126	0.115
GeH_5^-	1.717	1.558	0.086	0.075	0.117	0.132
SnH_5	1.854	1.747	0.076	0.109	0.098	0.170
SnH_5^-	1.896	1.799	0.072	0.138	0.087	0.173
CH_4	1.084	1.084	0.285	-1.052	0.285	-1.052
SiH_4	1.479	1.479	0.116	0.297	0.116	0.297
GeH_4	1.520	1.520	0.130	0.139	0.130	0.139
SnH_4	1.738	1.738	0.101	0.188	0.101	0.188

^aDistances are in Å; ρ and $\nabla^2\rho$ values are in au.

interested in relative energetics of these systems as opposed to the absolute values, and the former should be reliable. In reaction 1, which measures the electron affinity of MH_5 , the product is more stable than the reactants when $M = Si, Ge,$ and Sn . Interestingly, both SiH_5 and SnH_5 have a larger electron affinity than GeH_5 . Reaction 2 measures the hydrogen affinity of MH_4 . Here, the product is less stable than the reactants for all M , although there is a dramatic decrease in the endothermicity from C to the other group IV elements. Reaction 3 measures the hydride affinity of MH_4 and exhibits the same trend as noted for reaction 1. The anomalous behavior of Ge in reactions 1 and 3 may be related to the inert pair effect.²⁴ In general, the ΔH values (including zero-point vibrational corrections) exhibit the same trends as the ΔE values. Maitre and co-workers¹ emphasized the fact that reaction 3 is a destabilization reaction for C , whereas it is a stabilization reaction for Si and the heavier group IV elements. In section 4, we will examine these energy differences on an atomic level to gain a further understanding of the changes occurring upon complex formation.

3. Geometries and Critical Point Analysis. Table II lists the MH_{ax} and MH_{eq} internuclear distances. In all cases, for each system, $r(MH_{ax}) > r(MH_{eq})$. Further, $\Delta r = r(MH_{ax}) - r(MH_{eq})$ is greater for the anion than for the neutral species for a given M (with the exception of $M = Sn$). The largest Δr value (0.630 Å) is found for CH_5^- and the smallest (0.097 Å) is found for SnH_5^- .

Consistent with the shorter $r(MH_{eq})$ values is a greater accumulation of charge at the corresponding bond critical point. Further, for a given M , the larger MH distances in the anion correlate with a smaller value of $\rho(r_b)$ than in the corresponding radicals.

To further explore the redistribution of charge due to reaction 1, consider the density difference maps (Figure 1) in which the electron density of the radical is subtracted from the electron density of the anion at the anion geometry. In all systems, we see a greater accumulation of charge in the nonbonding regions of the axial hydrogens than the equatorial hydrogens, the difference being most pronounced in the $M = C$ systems. This observation is in accord with molecular orbital arguments, which suggest that the incoming electron will enter the radical HOMO of A_1' symmetry (which is essentially a nonbonding orbital centered on the two axial hydrogens) upon anion formation.

The redistribution of charge, as depicted in the density difference maps, also shows M losing electron density to the hydrogens as the electron is introduced. The quantitative density differences are given in Tables III–VI and are discussed in section 4 below.

Further examination of Table II reveals that for each penta-coordinated species, $\rho(r_b)$ for MH_{eq} is about the same as $\rho(r_b)$ for the corresponding MH_4 species. In each case, $\rho(r_b)$ for MH_{ax} is much smaller, since the axial hydrogens are bound by a weaker three-center-four-electron bond. Also compiled in Table II are $\nabla^2\rho(r_b)$ values. The CH bonds in CH_5 are covalent, based on the

Table III. Atomic Charges, First Moments, and Energies (in au) of MH_4 , MH_5 , and MH_5^- Systems

system	atom A	$q(A)$	$\mu(A)^a$	$E(A)$
CH_5	C	0.027	0.000	-37.6670
	H_{ax}	-0.060	-0.291	-0.5410
	H_{eq}	0.031	-0.114	-0.6179
CH_5^-	C	0.192	0.000	-37.5770
	H_{ax}	-0.602	-0.649	-0.5505
	H_{eq}	0.004	-0.135	-0.6370
CH_4	C	0.236	0.000	-37.6202
	H	-0.059	-0.118	-0.6455
SiH_5	Si	2.857	0.000	-287.9992
	H_{ax}	-0.434	0.227	-0.6669
	H_{eq}	-0.663	0.398	-0.7786
SiH_5^-	Si	2.989	0.000	-287.7544
	H_{ax}	-0.826	0.082	-0.7811
	H_{eq}	-0.779	0.292	-0.8074
SiH_4	Si	2.964	0.000	-287.9833
	H	-0.741	0.440	-0.8120
GeH_5	Ge	1.656	0.000	-2072.8541
	H_{ax}	-0.261	-0.016	-0.5961
	H_{eq}	-0.378	0.052	-0.6603
GeH_5^-	Ge	1.885	0.000	-2072.6110
	H_{ax}	-0.664	-0.201	-0.6850
	H_{eq}	-0.519	-0.026	-0.7019
GeH_4	Ge	1.776	0.000	-2072.8511
	H	-0.444	0.067	-0.6843
SnH_5	Sn	1.743	0.000	-5996.5325
	H_{ax}	-0.276	-0.002	-0.5604
	H_{eq}	-0.397	0.040	-0.6128
SnH_5^-	Sn	1.954	0.000	-5996.3454
	H_{ax}	-0.646	-0.141	-0.6481
	H_{eq}	-0.554	-0.049	-0.6471
SnH_4	Sn	1.840	0.000	-5996.5134
	H	-0.460	0.050	-0.6343

^aPositive (negative) signs denote direction of first moment is toward (away from) M.

Table IV. Changes in Atomic Charges (au), First Moments (au), and Energies (kcal/mol) for Reaction 1

M	atom A	$\Delta q(A)$	$ \Delta\mu(A) ^a$	$\Delta E(A)$
C	C	0.165	0.000	56.5
	H_{ax}	-0.542	-0.358	-6.0
	H_{eq}	-0.027	-0.021	-12.0
Si	Si	0.132	0.000	153.6
	H_{ax}	-0.392	-0.145	-71.7
	H_{eq}	-0.116	-0.106	-18.1
Ge	Ge	0.229	0.000	152.5
	H_{ax}	-0.403	-0.185	-55.8
	H_{eq}	-0.141	-0.078	-26.1
Sn	Sn	0.211	0.000	117.4
	H_{ax}	-0.370	-0.139	-55.0
	H_{eq}	-0.157	-0.089	-21.5

^aPositive (negative) signs denote that direction of the change of the first moment is toward (away from) M.

negative $\nabla^2\rho(r_b)$ values. Conversely, the SiH bonds in SiH_5 and SiH_5^- are ionic because the $\nabla^2\rho(r_b)$ values are positive. Owing to the large electronegativity difference between Si and H , an ionic

(24) Sidgwick, N. V. *The Electronic Theory of Valency*; Clarendon Press: Oxford, England, 1927; p 179.

Table V. Changes in Atomic Charges (au) and Energies (kcal/mol) for Reaction 2

M	atom A	$\Delta q(A)$	$\Delta E(A)$
C	C	-0.209	-29.4
	H _{ax}	-0.001	65.6
	H _{eq}	0.090	17.3
	H (ax attack)	-0.060	-26.5
	H (eq attack)	0.031	-74.7
Si	Si	-0.107	-10.0
	H _{ax}	0.307	91.0
	H _{eq}	0.078	21.0
	H (ax attack)	-0.434	-105.5
	H (eq attack)	-0.663	-175.6
Ge	Ge	-0.120	-1.9
	H _{ax}	0.183	55.3
	H _{eq}	0.066	15.1
	H (ax attack)	-0.261	-61.0
	H (eq attack)	-0.378	-101.3
Sn	Sn	-0.097	-12.0
	H _{ax}	0.184	46.4
	H _{eq}	0.063	13.5
	H (ax attack)	-0.276	-38.6
	H (eq attack)	-0.397	-71.5

Table VI. Changes in Atomic Charges (au) and Energies (kcal/mol) for Reaction 3

M	atom A	$\Delta q(A)$	$\Delta E(A)$
C	C	-0.044	27.1
	H _{ax}	-0.543	59.6
	H _{eq}	0.063	5.3
	H ⁻ (ax attack)	0.398	-39.8
	H ⁻ (eq attack)	1.004	-94.1
Si	Si	0.025	143.6
	H _{ax}	-0.085	19.4
	H _{eq}	-0.038	2.9
	H ⁻ (ax attack)	0.174	-184.5
	H ⁻ (eq attack)	0.221	-201.0
Ge	Ge	0.109	150.7
	H _{ax}	-0.220	-0.4
	H _{eq}	-0.075	-11.0
	H ⁻ (ax attack)	0.336	-124.2
	H ⁻ (eq attack)	0.481	-134.8
Sn	Sn	0.114	105.4
	H _{ax}	-0.186	-8.6
	H _{eq}	-0.094	-8.0
	H ⁻ (ax attack)	0.354	-101.0
	H ⁻ (eq attack)	0.446	-100.4

bond is formed between them. The $\nabla^2\rho(r_b)$ values are positive for the Ge and Sn systems as well.

$\nabla^2\rho(r_b)$ is the sum of the eigenvalues of the Hessian of $\rho(r_b)$. The curvature along the bond path, λ_3 , is the positive curvature, and in the systems explored here, this positive curvature (and $\nabla^2\rho(r_b)$ itself) increases in magnitude for the anionic MH bonds in the order C, Ge, Sn, and Si. Therefore, the most ionic bonds are the SiH bonds in SiH_5^- . Further evidence of ionicity is presented below.

4. Atomic Properties. The atomic properties necessary to explain the changes in electron density are the net charge on an atom in a molecule ($q(A)$), the first moment ($\mu(A)$), and the atomic energy ($E(A)$) described above.

An examination of the $q(A)$ column in Table III for $M = \text{Si, Ge, and Sn}$ neutral tetra- and pentacoordinated systems reveals the consequence of significant charge transfer from M to H, especially in MH_4 , and to H_{eq} in MH_5 . The largest transfers are for $M = \text{Si}$, suggesting the SiH bonds are the most ionic. For the corresponding anionic systems, there is even more electron density transferred from M to H than in the neutral systems, and the axial hydrogens acquire more electron density than the equatorial hydrogens. The increase in ionicity in the SiH bonds of the anion over the radical implies that the anion will be more stable than the radical (as evidenced in Table I). As the electronegativity differences between C and H are slight, the $q(A)$ observations apply to $M = \text{C}$ on a much smaller scale (with the exception of $q(\text{H}_{\text{ax}})$ in CH_5^-).

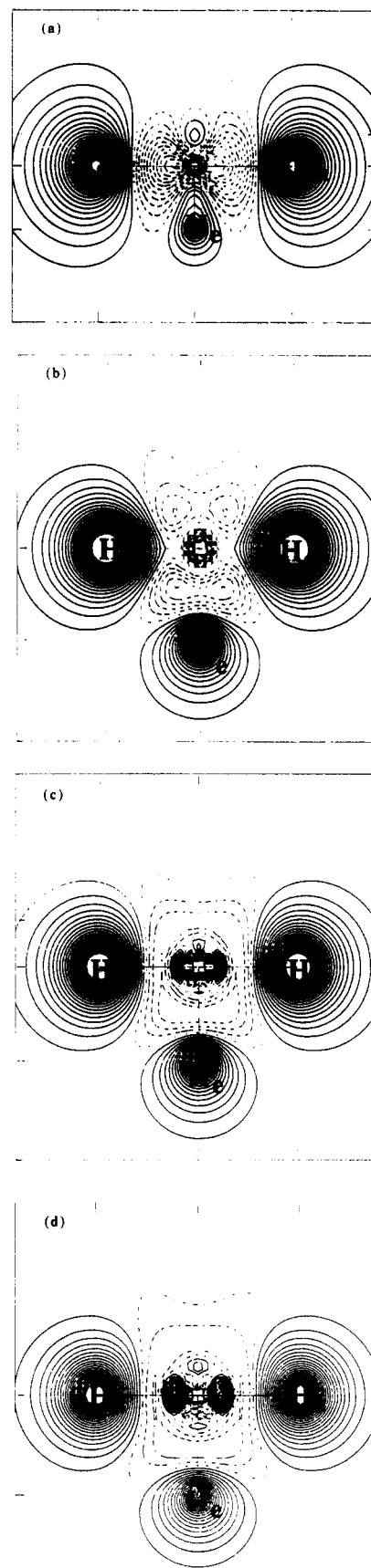


Figure 1. Density difference contour maps in the σ_v plane: $\rho(\text{MH}_5^-) - \rho(\text{MH}_5)$ at RHF geometry of the anion. Solid (dashed) lines correspond to electron density buildup (removal). The equatorial hydrogen in the σ_v plane is denoted by the symbol H_{e} , and the axial hydrogens are denoted by the symbol H_{a} . $M = \text{C, Si, Ge, and Sn}$ for parts a-d, respectively.

A perusal of the $\mu(A)$ column in Table III for $M = \text{Si, Ge, and Sn}$ MH_4 systems reveals that the electron density belonging to the hydrogen is polarized counter to the direction of the electron-density transfer and, therefore, toward the central atom. The polarization is greatest for H in SiH_4 as $q(\text{H})$ here is much larger in magnitude than it is in GeH_4 or SnH_4 . In general, similar conclusions are found for the corresponding neutral MH_5 systems. The $q(\text{H}_{\text{eq}})$ values are larger in magnitude than the $q(\text{H}_{\text{ax}})$ values, and so the electron density of H_{eq} is more easily polarized toward the central atom. The electron density of the hydrogens in SiH_5^- is polarized toward the highly positively charged Si, but the electron densities of the hydrogens in GeH_5^- and SnH_5^- are polarized away from the respective central atoms ($q(\text{Ge})$ and $q(\text{Sn})$ are both much smaller than $q(\text{Si})$). The hydrogens in CH_4 , CH_5 , and CH_5^- are polarized away from the carbon. The final column in Table III lists the $E(A)$ values. These values are used as input to subsequent tables listing atomic energy differences. Of course, energy differences lend themselves to chemical interpretations much more readily than do absolute energy values.

It is instructive to discuss changes in $q(A)$ values, first moments, and energies, so Table IV, which deals with the changes in atomic properties for reaction 1, is now discussed. First, note that the axial hydrogen gains the majority of the incoming electron distribution. The equatorial hydrogens also gain some of the incoming electron. The result is a shift in the MH bond critical points closer to M, a consequent reduction in the volume of M, and a consequent depletion of the electron density in M.

The directions of the changes in the atomic first moments listed in Table IV imply that the nonbonding regions of the axial hydrogens gain more electron density than the bonding regions. For example, in SiH_5 , the centroid of negative charge for $\mu(\text{H}_{\text{ax}})$ is directed toward M and the magnitude is 0.227 au. For the anion, the direction is the same but only of magnitude 0.082 au. Thus, the incoming electron distribution finally must be preferentially accumulated in the nonbonding region of H_{ax} . The density difference maps show this result (Figure 1). Similar observations are made for $\mu(\text{H}_{\text{eq}})$. It is noteworthy that the magnitude of the change in $\mu(\text{H}_{\text{ax}})$ increases monotonically as the change in $q(\text{H}_{\text{ax}})$ increases. The smallest change is for $M = \text{Sn}$ and largest is for $M = \text{C}$.

It has been shown that in many cases an atom will be stabilized (ΔE will be negative) when the atom gains electrons.¹⁷ This is the case in Table IV. All the M atoms lose electron density and are destabilized, the largest destabilization occurring for $M = \text{Si}$. The axial hydrogens, which gain the most electron density, are stabilized the most while the equatorial hydrogens are stabilized to a lesser extent when $M = \text{Si, Ge, and Sn}$. For the $M = \text{C}$ case, even though the axial hydrogen gains more electron density than the equatorial hydrogen, it is stabilized to a lesser extent. It may be that this is the reason why CH_5^- is unstable relative to $\text{CH}_5 + e^-$. (Recall that the sum of the energy changes in the individual atoms listed in Table IV equals the energy of reaction 1 listed in Table I.)

Table V lists the changes in atomic properties for reaction 2. As the hydrogen atom attacks MH_4 (ending up in either an axial or equatorial position), M gains electrons and becomes stabilized (especially $M = \text{C}$). The axial and equatorial hydrogens (originally of MH_4) lose electrons and become destabilized. The incoming hydrogen atom gains electrons (except for $M = \text{C}$, equatorial attack) and is stabilized. The incoming hydrogen gains

more electron density and is stabilized more if it ends up in an equatorial rather than an axial position in the product. Still, this stabilization along with the stabilization of M does not override the destabilization of the other hydrogens. The result is positive energies of reaction for all M.

Table VI lists the changes in atomic properties for reaction 3. As the hydride ion attacks MH_4 , M loses electrons (except for $M = \text{C}$) and M becomes destabilized. This is in contrast to the reaction 2 results. Consistent with the reaction 2 results is the stabilization of the incoming hydride anion. It is this stabilization that is the dominant factor in determining that the energy of reaction 3 is negative for $M = \text{Si, Ge, and Sn}$.

Conclusions

In response to the introductory questions, the main conclusions are as follows.

(1) In general, C-H bonds exhibit shared (covalent) interactions while Si-H, Ge-H, and Sn-H bonds are closed-shell (ionic) in nature. There is substantially more electron density located at the C-H bond critical points than at the others. The H in the C-H bonds withdraws only a negligible amount of electron density from C, but for the heavier systems, the H withdraws a significant amount of electron density from M. The evidence presented in this paper demonstrating the ionicity of the SiH bond in both SiH_5 and SiH_5^- , and its role in stabilizing the latter system, contrasts with the conclusion drawn by Maitre and co-workers.¹

(2) SiH_5^- is more stable energetically than SiH_5 because the axial and equatorial hydrogens are stabilized to a greater extent than the silicon is destabilized. The SiH bonds in the anion are more ionic than the SiH bonds in the radical. The connection between these two points is made by the stabilization (or destabilization) of the atoms in these species as a result of the redistribution of charge. Similar results are found for $M = \text{Ge, Sn}$. The carbon destabilization upon CH_5^- formation is greater than the stabilization of the hydrogens, and so CH_5^- is less stable than CH_5 .

(3) Upon addition of an electron to MH_5 to form MH_5^- , electron density becomes polarized to a greater extent in the axial hydrogen nonbonded regions than in the equatorial hydrogen basins. This is evidenced by the directions of the changes of the hydrogen first moments.

(4) Upon addition of H to MH_4 to form MH_5 , the incoming H and M are stabilized to a lesser extent than the axial and equatorial hydrogens are destabilized, resulting in a positive value for ΔE . Upon addition of H^- to MH_4 to form MH_5^- , the stabilization of the incoming hydride ion is dominant for $M = \text{Si, Ge, and Sn}$, resulting in a negative value for ΔE . When $M = \text{C}$, the destabilization of the atoms originally comprising CH_4 is greater than the stabilization of the incoming hydride ion and ΔE is positive.

Acknowledgment. The computations described in this work were performed on the North Dakota State University IBM 3090/120E vector computer, obtained in part with the aid of a joint study agreement between IBM and NDSU. This work was supported in part by grants from the National Science Foundation (CHE-8911911) and the Air Force Office of Scientific Research (90-0052).

Registry No. CH_5 , 54128-18-6; CH_5^- , 12316-54-0; SiH_5 , 28693-40-5; SiH_5^- , 41650-16-2; GeH_5 , 30937-33-8; GeH_5^- , 138541-66-9; SnH_5 , 138541-67-0; SnH_5^- , 138541-68-1.